

Theoretical research of inulin's pharmacological activity by combining DFT with concept DFT methods

W. Long*, Y.K. Li, J.X. Ma, Y.B. Wang

School of Chemistry and Chemical Engineering, University of South China, Hengyang Hunan, 421001 P.R. China.

Received October 16, 2014; Revised May 20, 2015.

The molecular parameters of glucose, pyran-fructose, furfuran-fructose and inulin molecules were investigated by the density functional theory B3LYP method on the 6-311+g(d, p) basis set level. The calculated results indicate that the molecular stability order is: furfuran-fructose > pyran-fructose > glucose > inulin. Using the concept DFT method we found that inulin has the maximum chemical potential, the minimum chemical hardness and the maximum electrophilic index. The Fukui function scanning shows that the C₂ atom of the inulin molecule has strong electron-losing ability, so it is the active site of the inulin molecule. The E_{BDE} calculations show that O₂-H is the easiest position which could be broken off because the bond energy is only 94.65 kcal·mol⁻¹, which is far less than the adiabatic ionization potential value. A reasonable theoretical model was established for the pharmacological activity of inulin.

Keywords: Pharmacological Activity, Inulin, DFT and DRFT, Fukui Function.

INTRODUCTION

There is currently a considerable interest in inulin due to its pharmacological activities [1-6]. Jerusalem artichoke, which is abundant in inulin, is a large-area plant in China. Many kinds of fungi also contain inulin. We found that the plant containing inulin is wild reproductive and highly adaptable, so inulin shows the unique advantage of high resistance to pest invasion. It is easy to reach bumper harvest without manual weeding and fertilization, which attracted many scientists' attention. Jerusalem artichoke tubers contain glucose and a large amount of inulin, which has better resist pest invasion owing to the magical ingredient. There are many experiments [7-10] about inulin in order to research its magical function, but no theoretical research about inulin has been reported so far.

The clinical pharmacology of non-toxic inulin includes blood detoxifying, diuretic, detumescent, antibacterial and antiphlogistic function, so it is widely used in the cure of diseases such as fever, diarrhea and many others [11,12]. It has a magical two-way regulating blood pressure function: when hypertensive patients are cured by inulin, it effectively reduces blood sugar concentration; when hypotensive patients are cured by inulin, it distinctly raises blood glucose concentration [13]. Stevioside (CAS number 57817-89-7) is a macromolecular system with the formula C₃₈H₆₀O₁₈

shown in Figure 1(a). Inulin can be obtained by hydrolysis of stevioside. Chi [14] found that inulin has good oxidation resistance and it can play selective catalytic function superior to that of free radicals as (•OH) and super oxide anion free radical as (O₂•) in the human body, but the real process is not clear. Nieto-Nieto [15] found that a small amount of inulin can greatly increase (from 13.93 to 22.98 kPa) the compressive stress of the gels prepared at pH 7 in order to increase the apparent protein concentration. Aidoo [16] pointed out that inulin and polydextrose mixtures could be used for sugar-free chocolate manufacture with satisfactory physicochemical properties when sweetened with stevia or thaumatin extracts. Hu [17] also made the important conclusion that inulin has good antioxidant activities against hydroxyl radicals (•OH), super oxide radicals (O₂•) and DPPH radicals (DPPH•). In short, there are a lot of experimental reports about inulin, and it is very essential to do some theoretical chemical research in order to explain its magical pharmacological activity.

Predicting drug activity by the theory of chemical simulation calculation have been widely reported [18,19]. We chose *D*-marigold sugar (CAS number 87-81-0, formula C₆H₁₂O₆) to research its pharmacological activity, which can be contrasted to glucose, pyran-fructose, fructose, and furfuran-fructose. We compared the differences in their pharmacological activity by the concept DFT activity index [20-21]. The charge scanning of the inulin molecule was done by the Fukui function [22], which can predict the active position and

* To whom all correspondence should be sent:
E-mail: usclw2013@163.com

many different abilities.

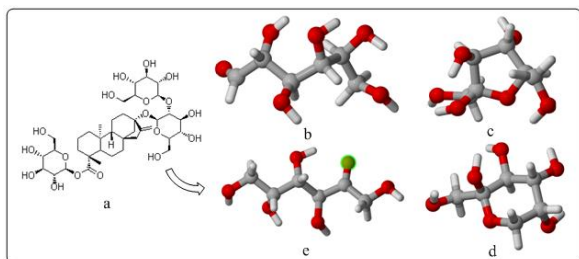


Fig. 1. Structure of the five molecules

THEORY AND CALCULATION METHODS

The geometry optimization of each species selected is carried out using DFT/B3LYP method with 6-311+g(d,p) basis sets [23]. The vibration frequencies are calculated at the B3LYP/6-311+g(d,p) level of theory for the optimized structure and the obtained frequencies are scaled by 0.9613 [24]. The other calculations are performed by the same method with the same basis set. We found that all vibration frequencies of each molecule are positive through vibration frequency analysis, which could certify that all calculated details are effective and credible.

In order to study the magical structure of the inulin molecule, taking into account the different solubility, we chose the PCM model solvent construction by water. At the same time, we performed molecular orbital analysis and charge distribution in the different systems. Also we obtained the charge value using natural bond orbital (NBO) analysis [25]. Density functional activity index is very effective in predicting the pharmacological activity and local selectivity [26]. In DFRT framework, the global reaction indices such as chemical potential μ and chemical hardness η are defined as:

$$\mu = -\chi = (\partial E / \partial N)_v$$

$$\eta = (\partial^2 E / \partial N^2)_v = (\partial \mu / \partial N)_v$$

E is the total energy of the system, N is the total number of electrons in the system, v is the external potential energy, μ can be defined as the negative value of electron negativity χ . According to the principle of Mulliken [27], $\mu = -\chi = -(I+A)/2$. Pearson [28] suggested that $\eta = I-A$, where I is the first ionization potential and A is the electron affinity. According to the closed shell theory, $I \approx -E_{\text{HOMO}}$ and $A \approx -E_{\text{LUMO}}$, where E_{HOMO} is the highest occupied molecular orbital energy, and E_{LUMO} is the lowest occupied molecular orbital energy. Parr and Liu [29] proposed the electric affinity index as $\omega = \mu^2 / 2\eta$, the force affinity index as $\Delta E_n = -A + \omega = (\mu + \eta)^2 / 2\eta$, and the electric affinity

index as $\Delta E_e = I + \omega = (\mu - \eta)^2 / 2\eta$.

Localized reaction index can be described by the Fukui function [29] which is the first order derivative between electron density (R) and the electron number (N). Because the Fukui function is discontinuous, we simplified the affinity electric Fukui function as $f^-(r)$, the affinity nuclear Fukui function as $f^+(r)$ and the free radical Fukui function as $f^0(r)$.

$$f(r) = (\partial \rho(r) / \partial N)_v$$

$$f^-(r) = \rho_{N(r)} - \rho_{N-1}(r)$$

$$f^+(r) = \rho_{N+1}(r) - \rho_{N(r)}$$

$$f^0(r) = (f^+(r) + f^-(r)) / 2$$

where $\rho_{N(r)}$ is the electron density of neutral molecules, $\rho_{N-1(r)}$ is the electron density of cation and $\rho_{N+1(r)}$ is the electron density of anion. We studied the chemical activity of hydroxyl in order to certify the better oxidation resistance of inulin. There are two kinds of molecular reaction mechanisms [30,31] about free radical scavenging tioxide ants: (1) in a nonpolar solvent, the straight pull hydrogen abstraction reaction could achieve the purpose, so the theoretical parameter is O-H bond dissociation energy (bond dissociation enthalpy, referred to as BDE); when E_{BDE} is lower, the reaction could take place more easily; (2) in a polar solvent, a proton-electron transfer reaction could take place and the theoretical parameter is the ionization potential (IP), when IP is lower, the reaction could take place more easily. As the human body is more complex, oxidation resistance performance of hydroxyl often need combine the measurement of E_{BDE} and IP parameters.

$$E_{\text{BDE}} = H_f + H_h - H_p = (\text{SPE}_f + \text{ZPVE}_f \times v + 3/2RT + 3/2RT + RT) + H_h - (\text{SPE}_p + \text{ZPVE}_p \times v + 3/2RT + 3/2RT + RT)$$

$$= (\text{SPE}_f + \text{ZPVE}_f \times v) + H_h - (\text{SPE}_p + \text{ZPVE}_p \times v)$$

$$\text{IP} = H_c - H_p$$

SPE is the electron energy, ZPVE is the zero point energy, v is a correction factor of 0.9804, H_p is the enthalpy of the parent molecule, H_h is the enthalpy of one hydrogen atom (0.49764 a.u.), H_f is the enthalpy of the free radical obtained when the parent molecule loses one hydrogen atom, H_c is the formation enthalpy of the radical cation in response. All calculations are done by the Gaussian 03 program [32]. Taking into account the really existent state of molecules, we have constructed the solvent model (PCM) with water as the solvent. Part of the images were analyzed and plotted through Gaussian-view, NBO and Multiwfn 2.5 program [33].

RESULTS AND DISCUSSION

Geometry Optimization

As shown in Figure 1, **a** is a stevioside molecule, **e** is a *D*-Marigold-inulin molecule obtained by hydrolysis from **a**, **b** is a glucose molecule, **c** is a pyran-fructose molecule, and **d** is a furfuran-fructose molecule. They all have hydroxyl groups, the molecular formula is $C_6H_{12}O_6$, and all of them can be dissolved in water and be absorbed into the cell. A carbon atom ring is involved in the **c** and **d** molecules, a carbonyl radical ($C=O$) in the **e** molecule, and an aldehyde radical ($-CHO$) in the **b** molecule. In order to compare the different molecular structures, we chose the B3LYP/6-311+g(d,p) method combined with the PCM solvent model (solvent is water) to optimize the molecular geometrical structure. We also analyzed the harmonic frequency vibration after the stable structure has been found. All results are positive which indicates that the molecular structure is stable.

As shown in Table 1 (the carbon atom number is shown in Fig.2), we found that the bond lengths in the four isomeric molecules are almost equal, the molecules are stable, and the C-C bond lengths in furan-fructose and pyran-fructose are the same as in the chain molecule, but the molecular intra angle is 110° . This is close to the straight chain molecule's angle of 119° , which leads to molecular stability. It is shown that the covalent radius of the carbon atom is 0.077 nm and the covalent radius of the oxygen atom is 0.066 nm [35], so the bond length of $C=O$ should be less than 0.143 nm. We found that the bond length of $C_1=O$ is 0.1200 nm in the **b** molecule, the bond length of $C_2=O$ is 0.1220 nm in the **e** molecule, both are less than 0.143 nm because of the different aldehyde radical effects. The bond angle data differing from 120° near the C_2 are due to the group electron attraction of the oxygen atom in the **e** molecule. As there are experimental results [36,37] for these molecules, we found that the error between calculated data and experimental data [35] is very small, so our calculations are credible and reasonable.

Infrared Spectroscopy

After single frequency analysis of the four molecules by the Gaussian 03 program [32], we found that all vibration frequencies are positive. The simple harmonic vibrations are attached by the Gauss-View program, we drew the infrared spectra of the four molecules as shown in Figure 3, and the

results are reasonable. Molecular vibration fingerprint peaks appeared between 400 and 1300 cm^{-1} due to the vibration of the total molecule. The absorption peaks between 1000 and 1400 cm^{-1} are due to the stretching vibration of the C-O bond in the molecules (including primary alcohol, secondary alcohol and tertiary alcohol). A strong absorption peak is observed at 1100 cm^{-1} in the **c** or **d** molecules due to the asymmetric stretching vibration of C-O-C bonds. A similar picture is observed for the **b** molecule. There is one strong absorption peak at 1700 cm^{-1} in the **e** molecule due to the vibration of the carbonyl $C=O$ bond, and several strong absorption peaks appeared at 2900 cm^{-1} in the **b** molecule due to the vibration of C-H bonds. There are some uncorrected results at a frequency about 2820 cm^{-1} . There are two areas of many small absorption peaks after 3000 cm^{-1} , which are mainly due to the expansion of C-H bond and the stretching of O-H bond.

NBO Analysis

In order to compare the atomic contribution in the four molecules, we performed atom charged scanning by the NBO program. The distribution of natural charges belonging to an atom is shown in Table 2. It is seen that both the C_1 atom in the **b** molecule and the C_2 atom in the **e** molecule show a strong positive charge owing to the strongly electronegative attraction of the oxygen atom in the $C=O$ bond. The atomic charge of the carbon atom is accounted for by the connected number of oxygen atoms and hydrogen atoms. The atomic charge of the C_5 atom is 0.5616e and 0.5492e in the **c** and **d** molecule, respectively, which is due to the lack of a hydrogen atom contributing a positive charge. The carbon atoms of the primary alcohol generally show more negative charges because of the steric effect, such as the C_6 atom in the **b** molecule and the C_1 atom in the **e** molecule. The oxygen atom shows a negative charge in all molecules. The maximum value of the negative charge has the oxygen atom attached to C_6 in the **b** molecule but not the oxygen atom in $C=O$, which is affected by the contribution of the electron cloud and the steric hindrance. The oxygen atom in C-O-C at both **c** and **d** molecules shows -0.6114e and -0.5560e respectively, which indicate that the connection tension between the ring atoms is suitable. The charge distribution may not explain the overall stability, and we have to judge by the natural orbit and the two-order perturbation stabilization energy, the related data are listed in Table 3.

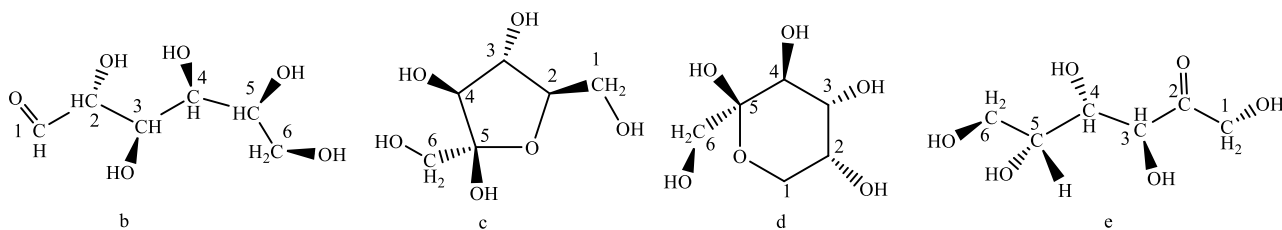


Fig. 2. The carbon atom number in the molecule.

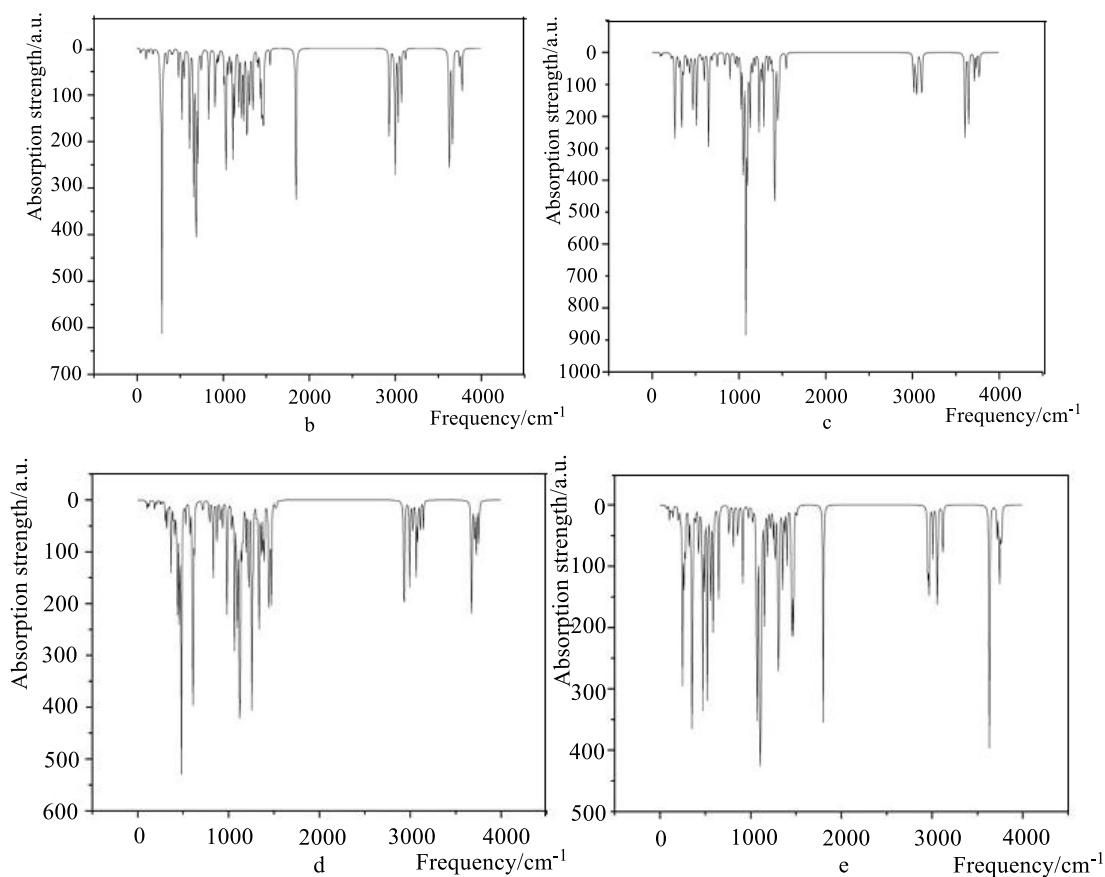


Fig. 3. Infrared spectra of the four molecules.

Table 1. Partial bond lengths (nm) and bond angle ($^{\circ}$) data.

Length	C ₁ -C ₂	C ₂ -C ₃	C ₃ -C ₄	C ₄ -C ₅	C ₅ -C ₆	C ₁ -O	C ₂ -O	C ₃ -O	C ₄ -O	C ₅ -O	C ₆ -O
b	0.1520	0.1550	0.1540	0.1550	0.1530	0.1200	0.1410	0.1430	0.1430	0.1430	0.1430
c	0.1530	0.1530	0.1540	0.1560	0.1530	0.1420	0.1450	0.1430	0.1410	0.1420	0.1430
d	0.1530	0.1530	0.1530	0.1550	0.1540	0.1430	0.1420	0.1420	0.1440	0.1430	0.1410
e	0.1520	0.1530	0.1550	0.1540	0.1530	0.1400	0.1220	0.1430	0.1410	0.1430	0.1420
Angle	$\angle(\text{O}-\text{C}_1-\text{C}_2)$	$\angle(\text{C}_1-\text{C}_2-\text{O})$	$\angle(\text{C}_1-\text{C}_2-\text{C}_3)$	$\angle(\text{C}_2-\text{C}_3-\text{O})$	$\angle(\text{C}_2-\text{C}_3-\text{C}_4)$	$\angle(\text{C}_3-\text{C}_4-\text{O})$	$\angle(\text{C}_3-\text{C}_4-\text{C}_5)$	$\angle(\text{C}_4-\text{C}_5-\text{O})$	$\angle(\text{C}_4-\text{C}_5-\text{C}_6)$	$\angle(\text{C}_5-\text{C}_6-\text{O})$	$\angle(\text{C}_5-\text{C}_6-\text{O})^*$
b	124.9	110.2	109.1	104.8	112.8	109.7	114.4	108.0	114.7	106.4	106.3
c	110.5	108.4	115.1	107.4	103.1	109.8	103.2	110.1	114.3	106.8	106.7
d	112.7	109.3	109.3	107.7	110.6	105.4	111.3	108.7	112.9	111.6	112.1
e	109.3	122.2	117.5	113.1	109.0	108.7	111.2	112.7	113.1	110.2	110.3

* from the experimental data in [34].

Table 2. Natural charge of atoms in the four molecules.

Molecule	C ₁	C ₂	C ₃	C ₄	C ₅	C ₆
b	0.3936	-0.0168	0.0635	0.0390	0.0351	-0.1281
c	-0.1043	0.0635	0.0462	0.0176	0.5616	-0.1252
d	-0.1199	0.0195	0.0474	-0.0063	0.5492	-0.1131
e	-0.1581	0.4679	-0.0238	0.0426	0.0423	-0.0981
Molecule	C ₁ -O	C ₂ -O	C ₃ -O	C ₄ -O	C ₅ -O	C ₆ -O
b	-0.5089	-0.7565	-0.7546	-0.7751	-0.7685	-0.7768
c	-0.7547	-0.6114	-0.7589	-0.7381	-0.7478	-0.7737
d	-0.5560	-0.7737	-0.7703	-0.7491	-0.7416	-0.7372
e	-0.7223	-0.4818	-0.7246	-0.7440	-0.7688	-0.7637

Table 3. Partial results by NBO analysis and the second-order perturbation energy.

Molecule	Donor NBO _(i)	Acceptor NBO _(j)	Stabilization energy E ₍₂₎ cal•mol ⁻¹
B	LP (C ₁ -O)	BD*C ₁ -C ₂	21.88
	LP (C ₁ -O)	BD*C ₁ -H	21.39
C	LP (C ₂ -O)	BD*C ₅ -O	12.95
D	LP (C ₃ -O)	BD*(C ₂ -O)-H	21.16
	LP (C ₁ -O)	BD*C ₅ -O	12.69
E	LP (C ₂ -O)	BD*C ₁ -C ₂	12.28
	LP (C ₂ -O)	BD*C ₂ -C ₃	11.26
	BD (C ₁ -H)	BD*(C ₃ -O)-H	10.22

If the two-order perturbation stabilization energy ($E_{(2)}$) is sourced from an isolated electron pair, this could indicate that the other repel force of bonds is small, so the molecular stability is high. The maximum value of $E_{(2)}$ is followed as Donor NBO_(i)→Acceptor NBO_(j). It is found that $E_{(2)}$ between the lone pair of electrons of the oxygen atom and the antibonding orbital has the maximum value in the **b**, **c**, **d** molecules which indicate that the three molecules are stable. $E_{(2)}$ value between the C₁-H bond and BD* of C₃-O-H in the **e** molecule is as large as 10.22 cal•mol⁻¹ and cannot be neglected. So the formation of molecular intra hydrogen bond on C₁-H in the **e** molecule may proceed under the effect of the oxygen atom attached to the C₃ atom. This influence may bring the inulin molecule in a stable state.

Molecular Energy and Frontier Orbit

In order to assess the different stability of the four molecules, we calculated the energy data at 0K which are listed in Table 4. We found that E_0 of the furan-fructose molecule has the lowest value, which is because the ring built of six atoms could better accommodate many electrons. The molecular energy data indicate that the furan-fructose molecule is the most stable one, the relative isomerism energy of the glucose molecule is 50.6721kJ•mol⁻¹, and the relative isomerism energy of the inulin molecule is 43.3208 kJ•mol⁻¹. The reason for this phenomenon is that the linear

molecule could cause molecular volume expansion, and the scope expansion of the electronic motion leads to an energy increase. In order to assess the electronic transitions and chemical energy, we calculated the energy level of the frontier molecular orbital, which is shown in Figure 4. HOMO is the highest molecular orbital, and LUMO is the lowest unoccupied molecular orbital. The HOMO-LUMO gap is used as a direct indicator of kinetic stability. A large HOMO-LUMO gap implies high kinetic stability and low chemical activity because it is energetically unfavorable to add electrons to a high-lying LUMO orbit [38] or to extract electrons from a low-lying HOMO orbit [39]. ΔE is the value of the HOMO-LUMO gap, and for lower ΔE the electron transition is easier and the molecule is more unstable.

It is shown that the inulin molecule is more unstable than the other ones because its $\Delta E=3.75\text{eV}$ which is the lowest value in Figure 4, and one electron could easily transit from the primary alcohols at the end of the molecule to the carbonyl bond (C=O), so the atom of the right hydroxy radical is the best active site which could easily lose one electron. The activity of the molecule is mainly controlled by the aldehyde radical which has a large contribution to the HOMO orbit and LUMO orbit. It is shown that the electronic transition of pyran-fructose is very difficult because its $\Delta E=7.51\text{eV}$ is the maximum energy gap among the others. The track comparison of LUMO orbit is dispersed,

covering the total pyran ring, which can indicate that the molecule has a better ability to accept electrons. Furan-fructose's frontier orbit is shown as **d** in Figure 4, the HOMO orbital distribution is relatively dispersed, and the value of ΔE is 6.81eV, so the electronic transition is not easy. LUMO orbital is almost contributed by the oxygen atom orbit which is connected to the C₄ atom. There is the same linear structure in the **b** and **e** molecules, but one aldehyde radical in the **b** molecule differs from that in the **e** molecule, so the energies are different in the **b** and **e** molecules. In contrast to the value of ΔE , we derived the stability of molecules as: $e < b < d < c$; the pyran-fructose molecule is the most stable one.

Table 4. Electronic energy, zero point energy and relative energy.

Molecule	$E_0(\text{a.u.})$	$E_{ZPE}(\text{a.u.})$	$E_{\text{tot}}(\text{a.u.})$	$\Delta E(\text{kJ}\cdot\text{mol}^{-1})$
b	-687.1257	0.1952	-686.9305	50.6721
c	-687.1446	0.1971	-686.9475	6.0387
d	-687.1478	0.1980	-686.9498	0
e	-687.1279	0.1946	-686.9333	43.3208

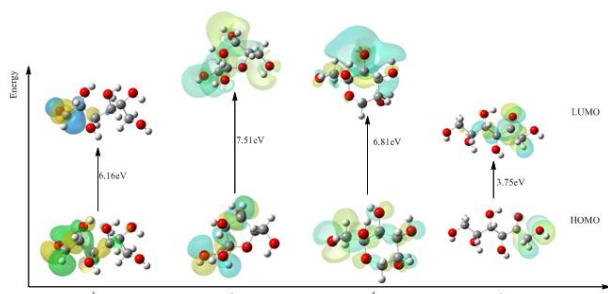


Fig.4. Diagram of the frontier orbital energy.

Concept DFT and Fukui Index Calculations

Recently, concept DFT active index (μ , η , ω , ΔE_n , ΔE_e) are applied widespread [20,21,40] both in inorganic and organic chemical field. If the molecule is in a transition state, the value of chemical potential μ would be the great, and the value of chemical hardness η would be small, so the molecule is in an unstable state. The opposite case is when the molecule is in a steady state, then the value of chemical potential μ would be small, and the value of chemical hardness η would be great. The electrophilic index ω could show the binding degree of a molecule with an electrophilic reagent, also the nucleophilic force differential index ΔE_n . The electrophilic force differential index ΔE_e is indicated as the activity degree of nucleophilic or electrophilic attack. All concept active indices are listed in Table 5. We found that the volume and the specific surface area of the **c** and **d** molecules decreased because of the formation of a cyclic

structure in the molecules, but the molecular volume and surface area of the **b** and **e** molecules are still large because of the straight chain. The order of the ionization potentials is $c > b \approx d > e$, and the ionization potential value of the inulin molecule is the lowest one. This conclusion is not the same as the former one, which is a result of not accurate correction. We also found that the same values of inulin's related indices are obtained using different methods, but this does not effect the final conclusion. Electron affinity values of **c** and **d** molecules are negative, which indicate that their energy would decrease after accepting one electron into the anion, but the electron affinity value of the **e** molecule is much larger than that of the **b** molecule, which could indicate that its energy would increase after accepting an electron into the anion and the stability of the anion has become weak. The chemical potential μ of the **e** molecule is the maximum one and the chemical hardness η is the lowest sample, which could certify that the **e** molecule is in a relatively stable state; the chemical potential μ of the pyran-molecule is lower and the chemical hardness η is maximal, which is probably because the whole molecule structure is unstable and the tension of the ring is so large that it could easily accommodate electrons. The electrophilic index ω of the **e** molecule is maximal, which points to its best activity and better electrophilic capability. Comparing ΔE_n and ΔE_e , we found that the value of ΔE_n of the **e** molecule is the maximal and the value of ΔE_e of the **e** molecule is the minimum, so the inulin molecule has better nucleophilic ability and it can become a good antioxidant drug.

In order to comprehensively understand the molecular activity, we performed local atomic Fukui index calculation on the inulin molecule, and the results are listed in Table 6. Obviously, the $f_{(r)}^-$, $f_{(r)}^+$, $f_{(r)}^0$ values of the six carbon atoms in the inulin molecule are different. The $f_{(r)}^+$ value of the C₂ atom is maximal, so its ability of gaining one electron is stronger than that of the other atoms, while the $f_{(r)}^+$ values of the C₄, C₅, C₆ atoms are negative, i.e., gaining one electron is impossible. The $f_{(r)}^-$ value of the C₂ atom is maximal, i.e., losing one electron is easy, so all carbon atoms except the C₃ atom could lose one electron. In contrast to the $f_{(r)}^+$ value, the electronic contribution is more distinct, the total molecule could easily lose one electron. Analysis of the $f_{(r)}^0$ values of all carbon atoms showed that the most active position is at the C₂ atom. Both $f_{(r)}^-$ value and $f_{(r)}^+$ value of the oxygen atom attached to the C₆ atom are the maximal, so it is able to easily capture one electron. The $f_{(r)}^+$ value of the oxygen atom attached to the C₂ atom is the

Table 5. Concept DFT indices of the four molecules.

Molecule	V Bohr ³	SA Bohr ²	I eV	A eV	μ eV	η eV	ω eV	ΔE_n eV	ΔE_e eV
b	1358.18	707.21	6.52	0.36	3.44	6.16	0.96	7.48	0.60
c	1287.23	669.13	6.72	-0.77	3.48	7.49	0.81	8.03	1.07
d	1313.91	666.31	6.50	-0.29	3.11	6.79	0.71	7.22	1.00
e	1329.88	708.32	6.45	2.71	4.58	3.74	2.80	9.25	0.09

Table 6. Fukui function analysis of key atoms in the inulin molecule.

Atom	$\rho_{N(r)}$	$\rho_{N-1(r)}$	$\rho_{N+1(r)}$	$f^-(r)$	$f^+(r)$	$f^0(r)$
C ₁	0.1581	0.1698	0.1448	0.0117	0.0133	0.0125
C ₂	0.4679	0.5677	0.1925	0.0998	0.2754	0.1876
C ₃	0.0238	0.0023	0.0088	-0.0215	0.0150	-0.0033
C ₄	0.0426	0.0731	0.0701	0.0305	-0.0275	0.0015
C ₅	0.0423	0.0457	0.0490	0.0034	-0.0067	-0.0017
C ₆	0.0981	0.1264	0.1081	0.0283	-0.0100	0.0092
C ₁ -O	0.7223	0.7123	0.7316	-0.0100	-0.0093	-0.0097
C ₂ -O	0.4818	0.3757	0.7650	-0.1061	-0.2832	-0.1947
C ₃ -O	0.7246	0.7175	0.7908	-0.0071	-0.0662	-0.0367
C ₄ -O	0.7440	0.6914	0.8052	-0.0526	-0.0612	-0.0569
C ₅ -O	0.7688	0.7348	0.7926	-0.0340	-0.0238	-0.0289
C ₆ -O	0.7637	0.5236	0.7756	-0.2401	-0.0119	-0.1260

Table 7. E_{BDE} energy of the different hydrogen atoms

Molecule	SPE_f (a.u.)	ZPV_p (kJ•mol ⁻¹)	O—H E_{BDE} (kJ•mol ⁻¹)
	-687.127937	511.068278	—
1-H	-686.459871	470.287437	407.471927
2-H	-686.465734	474.290536	396.003258
3-H	-686.454712	473.926642	424.585545
4-H	-686.459414	473.009817	411.340801
5-H	-686.456683	471.023627	416.563519

lowest one so that it is difficult for the C₂ atom to accept one electron but it could lose one electron, which makes the inulin's real molecular structure magical.

Evaluation of the Antioxidant Ability

In pharmacological aspect, the inulin molecule shows very good antioxidant properties [41,42]. It is known that inulin could exert pesticide effect by reacting with the hydroxyl free radical ($\bullet OH$) or the super oxide anion free radical ($O_2\bullet$). The reaction mechanism of disposal of free radicals mainly depends on the role of hydroxyl dehydrogenation, which could be assessed by the E_{BDE} and IP parameters. Therefore, we calculated the E_{BDE} value of the different hydrogen atoms on the basis of the molecular stable structure which has been optimized by the B3LYP method. Every hydrogen atom in the inulin molecule is numbered as shown in Figure 5, and the E_{BDE} values of the different

hydrogen atoms are listed in Table 7.

It is shown that the E_{BDE} values of hydrogen atoms at different positions are different. When the E_{BDE} value is lower, this position can more easily provide a hydrogen atom, so the antioxidant ability is stronger. We found that 2-H is most easily broken because its E_{BDE} value is the lowest one, which is due to the strong electronic contribution of carbonyl (C=O). But the E_{BDE} value of the 3-H atom is by approximately 28.5800 kJ•mol⁻¹ higher than that of the 2-H atom. We calculated the vertical ionization energy and the adiabatic ionization energy of the inulin molecule by the same method, the values are 196.5600 kcal•mol⁻¹ and 183.1500 kcal•mol⁻¹, respectively. Both ionization energies are very high, so the E_{BDE} value is reasonable to explain the antioxidant activity.

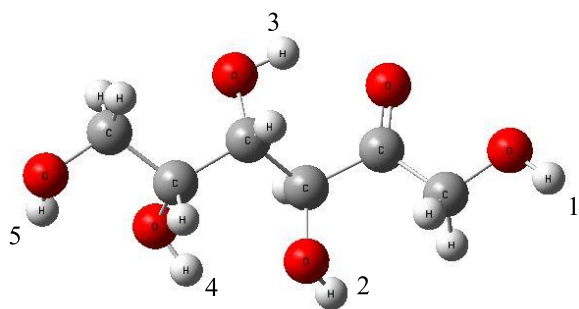


Fig.5. Hydrogen atom numbers in the inulin molecule.

CONCLUSIONS

We found that the stability order is furan-fructose>pyran-fructose>glucose>inulin through geometrical structure optimization, frequency analysis, infrared spectroscopy, atom charge population, NBO analysis, and frontier orbital energy calculation by the DFT method. On this basis, we chose the concept DFT activity index method to analyze the various parameters of inulin molecule. The chemical potential and the electrophilic index of the inulin molecule are great, but the chemical hardness is small. The C₂ atom is the active center of the whole molecule because it is the easiest position for losing one electron through the Fukui index scanning. Calculations of E_{BDE} showed that 2-H is the most easily broken off position because the value is far less than the adiabatic ionization potential. All these can form a reasonable theoretical model to explain the magical pharmacological activity of the inulin molecule.

REFERENCES

1. H.Y. Zhang, L.F. Wang, Y.M. Sun, *Bioorganic & Medicinal Chemistry Letters*, **13**, 909 (2003).
2. J.H. Roe, J.H. Epstein, N.P. Goldstein, *J. Biol. Chem.*, **178**, 839 (1949).
3. Y. Zhang, T.H. Chen, J.T. Sun, *Chemistry Bulletin*, **65**, 12 (1998).
4. G.R. Gibson, E.R. Beatty, X. Wang, *Gastroenterology*, **108**, 975 (1995).
5. R.A.A. Muzzarelli, J. Boudrant, D. Meyer, *Carbohydrate Polymers*, **87**, 995 (2012).
6. S. Stoyanova, J. Geuns, E. Hideg, *Int. J. Food Sci. & Nutr.*, **62**, 207 (2011).
7. P. Andrewes, J.L.H.C. Busch, T. Joode, *J. Agric. & Food Chem.*, **51**, 1415 (2003).
8. K. Seki, K. Haraguchi, M. Kishimoto, S. Koboyashi and K. Kainuma, *Agric. Biol. Chem.*, **53**, 2089 (1989).
9. Y.J. Zhang, *Anal. Chem.*, **5**, 167 (1977).
10. Y.M. Sun, H.Y. Zhang, D.Z. Chen, *Org. Letters*, **4**, 2909 (2002).
11. J. Luo, S.W. Rizkalla, C. Alamowitch, *Am. J. Clin. Nutr.*, **96**, 939 (1996).
12. M.L. Jose, T. Elad, P. Raymond, D.M. Glahn, *Food Chem.*, **109**, 122 (2008).

13. K.G. Jackson, G.R. Taylor, A.M. Clohessy, *Brit. J. Nutrition*, **82**, 23 (1999).
14. Z.M. Chi, T. Zhang, T.S. Cao, *Biol. Tech.*, **102**, 4295 (2011).
15. T.V. Nieto-Nieto, Y.X. Wang, L. Ozimek, L.Y. Chen. *Food Hydrocolloids*, **50**, 116 (2015).
16. R.P. Aidoo, E.O. Afoakwa, K. Dewettinck. *LWT-Food Science and Technology*, **62**, 592 (2015).
17. Y.X. Hu, J. Zhang, C.W. Yu, Q. Li, F. Dong, G. Wang, Z.Y. Guo. *International Journal of Biological Macromolecules*, **70**, 44 (2014).
18. L.J. Pauling, *J. Am. Chem. Soc.*, **62**, 2643 (1940).
19. M. Azenha, P. Kathirvel, P. Nogueira, *Biosens. & Bioelectron.*, **23**, 1843 (2008).
20. A.D. Becke, *J. Chem. Phys.*, **97**, 9173 (1992).
21. R.G. Parr, W. Yang, *J. Am. Chem. Soc.*, **106**, 4049 (1984).
22. K. Fukui, *J. Phys. Chem.*, **74**, 4161 (1970).
23. M.P. Andersson, P. Uvdal, *J. Phys. Chem. A*, **109**, 2937 (2005).
24. A.P. Scott, L. Random, *J. Phys. Chem.*, **100**, 16502 (1996).
25. M. Szafram, A. Komasa, E.B. Adamska, *J. Mol. Struct.*, **827**, 101 (2007).
26. B. Miehlich, B., A. Savin, A., H. Stoll, H. Preuss, *Chem. Phys. Letters*, **157**, 200 (1989).
27. Y. Li and J.N.S. Evans, *J. Am. Chem. Soc.*, **117**, 7756 (1995).
28. R.G. Pearson, Springer-Verlag: Berlin, **22**, 101 (1993).
29. S.B. Liu, *Acta Phys.-Chim. Sin.*, **25**, 590 (2009).
30. G.T. Head, G.M. Head, M.J. Frisch, *J. Am. Chem. Soc.*, **113**, 5989 (1991).
31. R.B. Ammar, W. Bhourri, M.B. Sghaier, *Food Chem.*, **116**, 258 (2009).
32. M.J. Frisch, G.W. Trucks, H.B. Schlegel, Gaussian 03, Revision D.02; Gaussian Inc.: Pittsburgh, PA, 2003.
33. T. Lu, F.W. Chen, *J. Comp. Chem.*, **33**, 580 (2012).
34. M.Z. Saavedra-Leos, C. Leyva-Porras, E. Martínez-Guerra, S.A. Pérez-García, J.A. Aguilar-Martínez, C. Álvarez-Salas. *Carbohydrate Polymers*, **105**, 10 (2014).
35. J.A. Dean Ed. Lang's Handbook of Chemistry, Thirteenth Edition. McGraw-Hill Book Company, 1985.
36. L. Santiago-Rodríguez, M. M. Lafontaine, C. Castro, J. Méndez Vega, M. Latorre-Esteves, E. J. Juan, C. Rinaldi, *J. Mater. Chem. B*, **22**, 2807 (2013).
37. K.D.O. Vigier, A. Benguerba, A. Barrault, *J. Green Chem.*, **14**, 285 (2012).
38. F. Russo, C. Clemente, M. Linsalata, M. Chiloiro, A. Orlando, E. Marconi, *Europ. J. Nutr.*, **50**, 271 (2011).
39. R.M. Yosadara, *J. Phys. Chem., A*, **106**, 11283 (2002).
40. P. Geerlings, F. Deproft, W. Langenaeker, *Chem. Rev.*, **103**, 1793 (2003).
41. E.M. Dewulf, P.D. Cani, A.M. Neyrinck, *J. Nutr. Biol. & Chem.*, **22**, 712 (2011).
42. B.S. Reddy, R. Hamid, C.V. Rao, *Carcinogenesis*, **18**, 1371 (1997).

ТЕОРЕТИЧНО ИЗСЛЕДВАНЕ НА ФАРМАКОЛОГИНАТА АКТИВНОСТ НА ИНУЛИН ЧРЕЗ КОМБИНАЦИЯ НА DFT С КОНЦЕПТУАЛНИ DFT-МЕТОДИ

В. Лонг*, И.И. Ли , Дж.С. Ма, И.Б. Ванг

Училище по химия и химично инженерство, Южнокитайски университет, Хенгян, Юнан, 421001 Китай

Постъпила на 16 октомври, 2014 г.; Коригирана на 20 май, 2015 г.

(Резюме)

Молекулните параметри на глюкозата, пирано-фруктозата, фурфуран-фруктозата и на инулина са изследвани с помощта на DFT –теорията по метода B3LYP на базата на 6-311+g(d, p)–ниво. Изчислителните резултати показват, че редът на молекулна стабилност е: фурфуран-фруктоза>пиран-фруктоза>глюкоза>инулин. С помощта на концептуален DFT-метод намерихме, че инулинът има максимален химичен потенциал, минимална химическа устойчивост и максимален електрофилен индекс. Сканирането чрез функция на Fukui показва, че C₂-атомът в инулиновата молекула има силна склонност към отдаване на електрони и затова е активната ѝ част. E_{BDE} –изчисленията показват, че връзката O₂-H е най-лесна за разкъсване понеже енергията ѝ е само 94.65 kcal•mol⁻¹, което е много по-малко от потенциала за адиабатична йонизация. Съставен е подходящ теоретичен модел за фармакологичната активност на инулина.